# Electronic Supplementary Information (ESI)

## Electrolyte Engineering Enables High Energy Li||CF$_x$ Battery Operation at Ultralow Temperatures

Weijing Yang,[a,d] Xuyang Chen,[b] Baoyu Sun,[c,*] Bin Zhang,[d] Shangde Ma,[d] Yang Dai,[e,*] Quansheng Zhang,[b] Junliang Zhang,[a,*] Jingying Xie[d,*]

[a] Institute of Fuel Cells, Shanghai Jiao Tong University, Shanghai 200240, China;

[b] School of Chemical and Environmental Engineering, Shanghai Institute of Technology, Shanghai 201418, China;

[c] State Key Laboratory for Mechanical Behavior of Materials, Shaanxi International Research Center for Soft Matter, School of Materials Science and Engineering, Xi'an Jiaotong University, Xi'an 710049, China;

[d] State Key Laboratory of Space Power-Sources, Shanghai Institute of Space Power-Sources, Shanghai 200245, China;

[e] Department of Chemical Engineering，Shanghai University, Shangda Road 99, Shanghai, 200444, China.

* Corresponding author E-mail: Baoyu.Sun@xjtu.edu.cn (B.Sun), dy1982@shu.edu.cn (Y.Dai), junliang.zhang@sjtu.edu.cn (J.Zhang), jyxie@hit.edu.cn (J.Xie).

## Experimental Section

**Electrolyte preparation:** 1.0 M $LiBF_4$ Propylene Carbonate (PC)/1,2-Dimethoxyethane (DME) 1:1 v/v, Lithium Tetrafluoroborate ($LiBF_4$, 99.9%) were sourced from DodoChem. Ethyl acetate (EA, 99.5%, Aladdin), Ethyl trifluoroacetate (TFAE, 99%, Aladdin) and Fluoroethylene Carbonate (FEC, 98%, Aladdin) were dried with 4 Å molecular sieves before employing. EA/ET-based electrolytes are prepared by blended 1.0 M $LiBF_4$ molar ratio with EA/ET in volume, respectively.

The procedures were carried out Mikrouna universal glovebox ($O_2$<0.1ppm, $H_2O$<0.1 ppm). The ionic conductivity was tested by Electrochemical impedance spectroscopy (EIS) on a Potentiostat/Galvanostat (Solartron 1260+1287, 10 mV,1 MHz to 0.01 Hz).

**Material characterization:** SEM images of the cycled electrodes (lithium anodes and S-NMC811 cathodes), were investigated by scanning electron microscope (SEM) (ZEISS Sigma 300). XRD (Rigaku Smart Lab SE) was employed to test the cycled S-NMC811cathode. The Raman spectra was observed on Horiba LabRam HR Evolution. XPS spectra (Thermo Scientific K-Alpha+ with an Al Kα radiation (1486.6 eV)) were applied to probe the cycled S-NMC811 cathode. All the XPS tests were performed in a home-made air-free capsule between the glovebox and instruments.

**Preparation of cathodes:** $CF_x$ material (Zuoxi Hubei, China), conductive carbon, Super-p, VGCF and PVDF (80/10/10 % in weight) were carefully grinded, then stirred in N-Methyl-2-pyrrolidone (NMP) to generate a uniform slurry. After that, the slurry was coated on a C-coated aluminum foil (Showa Denko Corp.) and then dried at 80°C for 24 h in vacuum. The 1C-rate was determined as 800 mA $g^{-1}$. Then the dried foil was cut into coin-shaped electrodes, with an active mass loading of 2-3 mg $cm^{-2}$. The 2032-shaped coin cell was assembled with $CF_x$ cathode, separator (Celgard 2400), and Li foil in glovebox. The cycled cathode and lithium metal were carefully dissembled and rinsed with Dimethyl carbonate (DMC) and dried in glovebox. The electrochemical performance was tested using the Land CT2001A until 1.5 V at room temperature and low temperature in a freezer (DW-HL100, Zhongke Meiling Cryogenics Co.,Ltd), respectively. The EIS is tested on Solartron 1260+1287 (10 mV, 1 MHz to 0.01 Hz) after the various cycles. The dry18650 cells were purchased from Shandong Zhongshan Photoelectric Materials Co., Ltd. with the high voltage $CF_x$ material (~3.05 V). The dry cells were filled with the various electrolytes and sealed in a dry room.

**Molecular dynamic simulation**: The molecular structures of the components were first optimized. The calculation results were obtained by using the first-principal method through the Density Functional for Molecules, version 3 (DMol3) module in Materials Studio. The calculations were performed using the density functional theory (DFT) with the Perdew-Burke-Ernzerhof (PBE) functional based on generalized gradient approximation (GGA) and the projector-augmented wave (PAW) method. The cutoff energy of atomic wave functions is set to be 630 eV. The k point is set to be 2 × 2 × 2. The atom positions are relaxed using the Broyden-Fletcher-Goldfarb-Shanno (BFGS) method. All structures are fully relaxed without any symmetrical constraint. The structural optimization parameters are Energy, Max. force and Max. displacement, which are set to 1.0 e-5 eV/atom 0.03 Ha/Å and 0.001 Å, respectively.

The molecular dynamics (MD) simulations were employed to investigate the $Li^+$ solvation structures of the BE, and 1M $LiBF_4$ EA/ET 7/3 v/v electrolytes. The BE model contains 20 $LiBF_4$, 140 DME, and 120 PC molecules. The 1.0 M $LiBF_4$ EA/ET 7/3 v/v model contains 20 $LiBF_4$, 120 ET, 60 EA molecules. The molecular dynamics (MD) simulations were performed using a running time of 500 ps with a 1 fs time step. Under the Universal forcefield, the canonical ensemble (NVT) was applied to allow the system to exchange heat with the environment, while the constant temperature (298 K and 233 K) was controlled by the Nose method. The simulation time was set to be long enough to ensure that the electrolyte system reaches equilibrium.

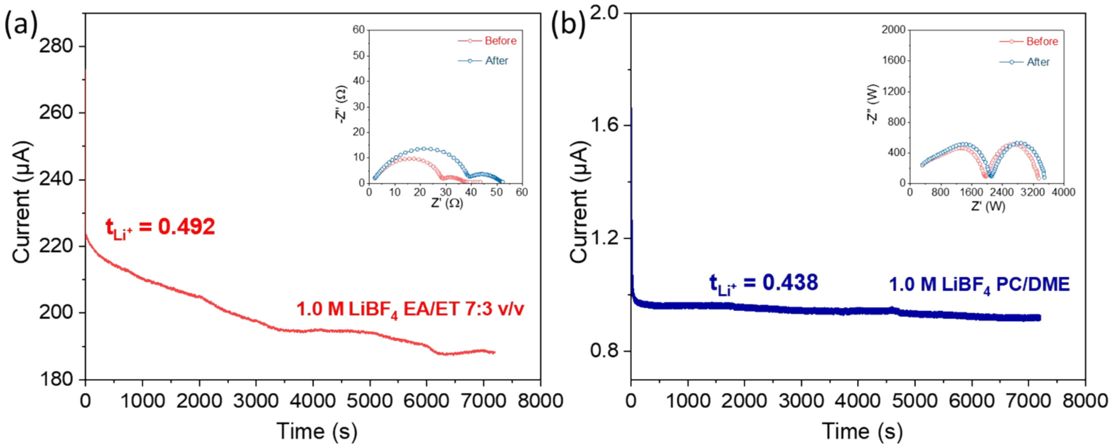

**Fig. S1.** The DC polarization curve and (inset) electrochemical impedance spectra of the Li symmetric battery with (a) 1M LiBF$_4$ EA/ET 7:3 v/v (b) Baseline, respectively.

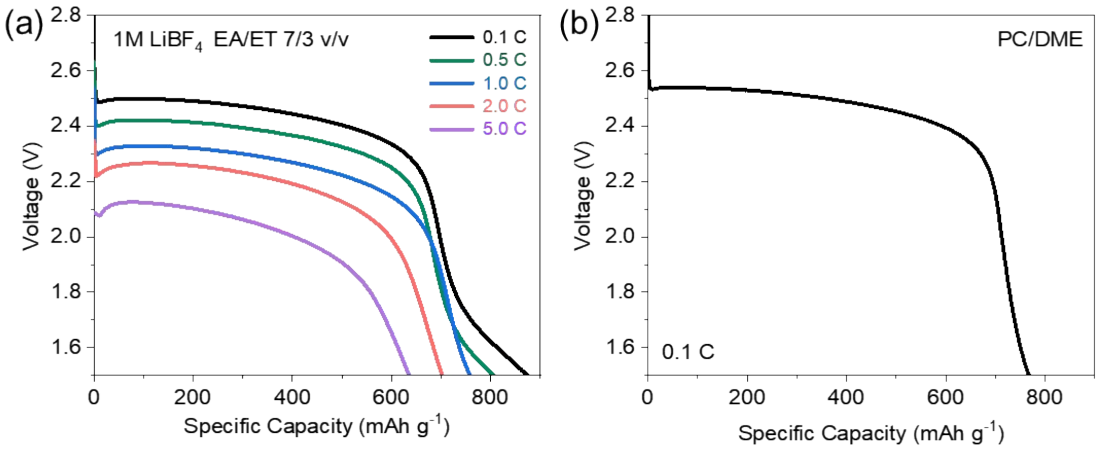

**Fig. S2.** (a) Discharge profiles of the cells with EA/ET electrolyte at different rate currents, and (b) the cell with PC/DME electrolyte at 0.1 C.

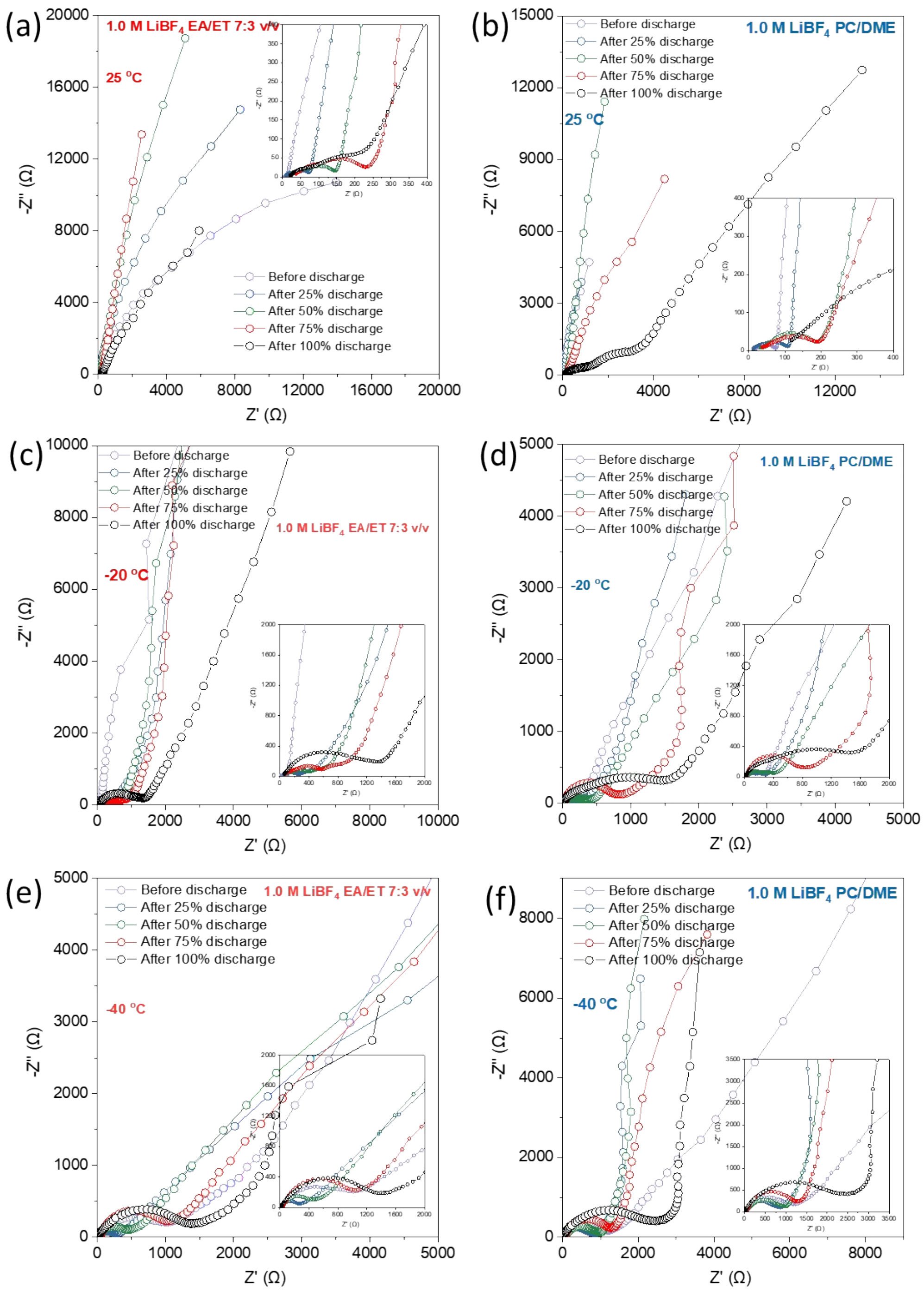

**Fig. S3.** EIS spectra and related equivalent circuit of the cells used PC/DME and EA/ET electrolyte under different temperature and during different stages of discharge, respectively. Cells discharge with 1.0 M $LiBF_4$ EA/ET 7:3 v/v electrolyte at (a) 25°C, (c) -20°C, and (e) -40°C，and the baseline electrolyte (1.0 M $LiBF_4$ PC/DME) at (b) 25°C, (d) -20°C, and (f) -40°C.

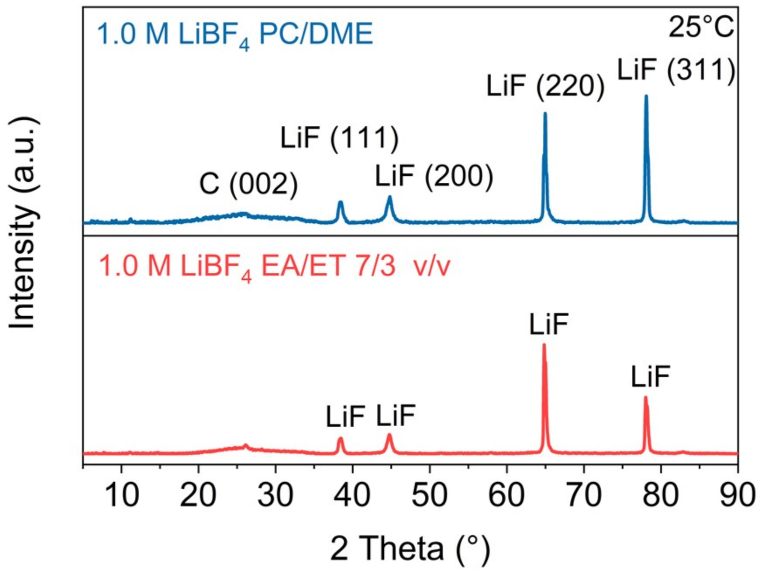

**Fig. S4.** XRD spectra of the discharged $CF_x$ cathodes used PC/DME and EA/ET electrolyte at room temperature.

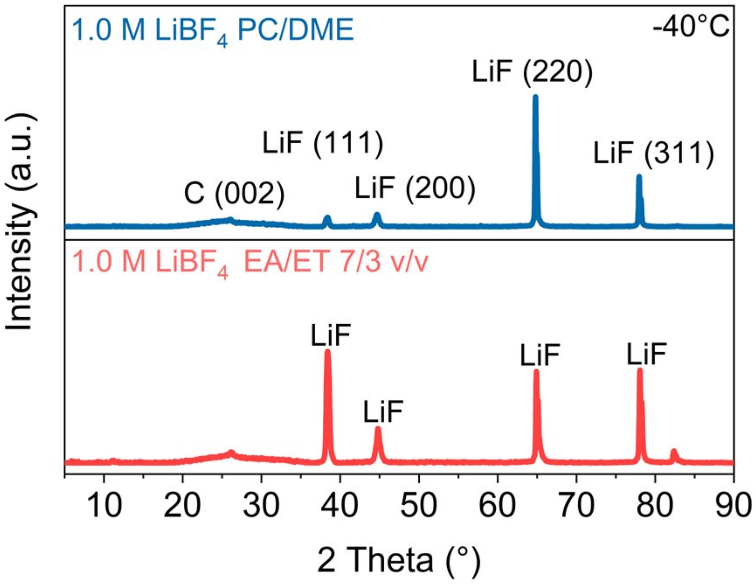

**Fig. S5.** XRD spectra of the discharged $CF_x$ cathodes used PC/DME and EA/ET electrolyte at the operation temperature of -40 °C.

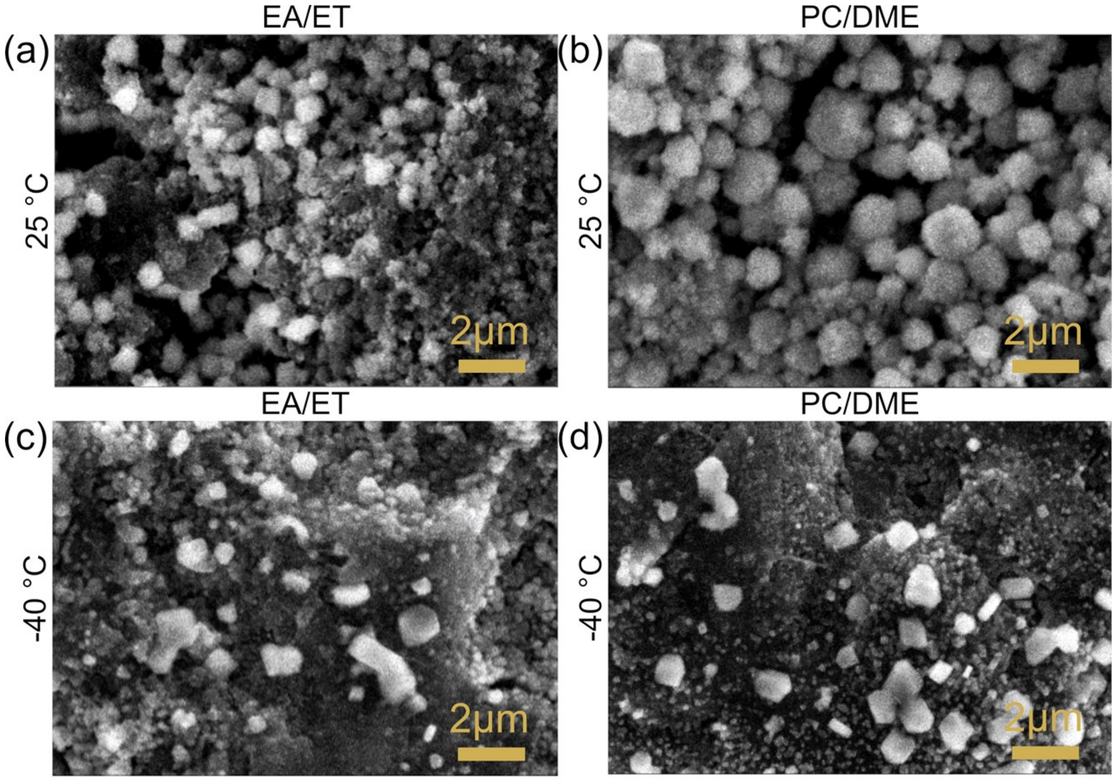

**Fig. S6.** SEM images of the cycled electrodes with (a, c) EA/ET and (b, d) PC/DME at 25 °C and -40 °C, respectively.

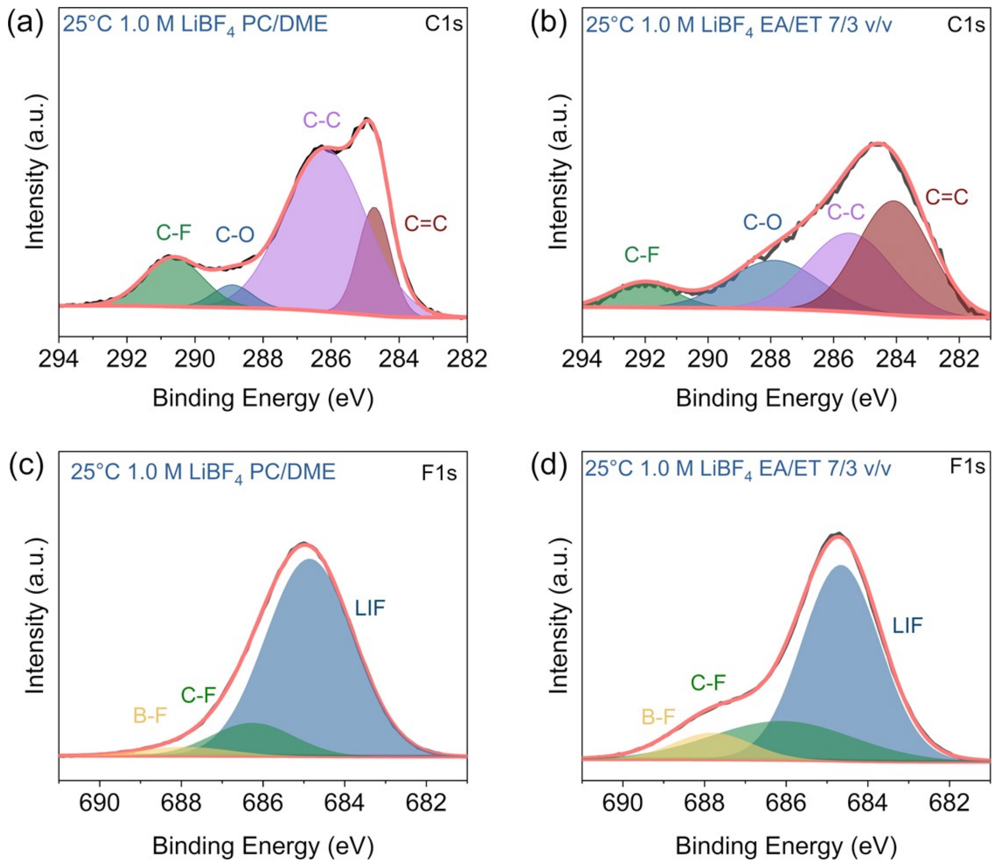

**Fig. S7.** XPS C1s spectra and XPS F1s spectra of the discharged $CF_x$ cathode used (a, c) PC/DME and (b, d) EA/ET electrolyte at room temperature, respectively.

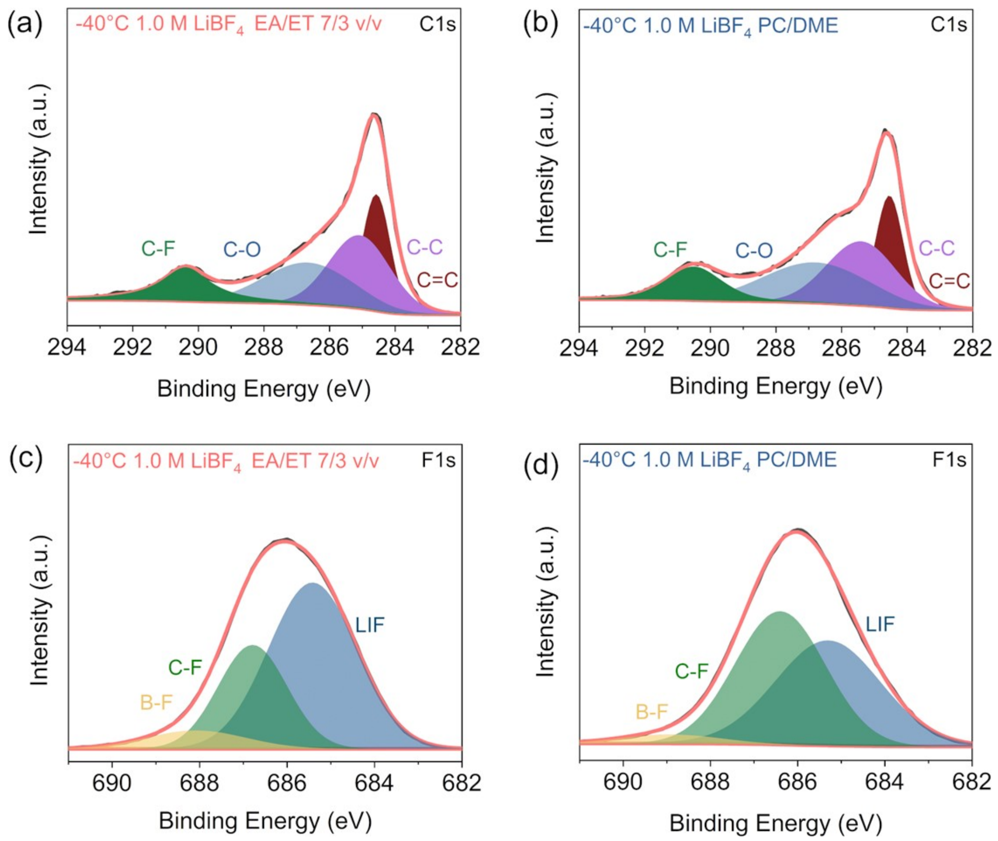

**Fig. S8.** XPS C1s spectra and XPS F1s spectra of the discharged $CF_x$ cathode used (a, c) EA/ET and (b, d) PC/DME electrolyte at -40 °C, respectively.

**Table S1.** Comparison of the low temperature performance CFx/Li batteries

| Electrolyte | Temperature (°C) | Current density (mA $g^{-1}$) | Capacity (mAh $g^{-1}$) and cutoff (V) | Active mass loading (mg/$cm^{-2}$) | $E_{1/2}$ Plateau voltage (V)* | Reference |
|---|---|---|---|---|---|---|
| 0.3M LiTFSI THF/CO2/FM = 1:4:95 vol%) | -40 | 10 | 600, 0.5 | / | 1.6 | S1[1] |
| 0.5 M $LiBF_4$/Acetonitrile: γ-butyrolactone | -50 | 16 | 350, 1.5 | / | 1.7 | S2[2] |
| 1M LiFSI in 1: 2 PC/ Methyl Butyrate v/v | -40<br>-60 | 80 | 820, 0.5<br>370, 0.5 | 1~2 | 2.0<br>1.6 | S3[3] |
| 1 M $LiBF_4$ in γ-butyrolactonewith 2 vol% 15-crown-5 additive | -40 | 6.67 | 50, 0.5 | / | 1.6 | S4[4] |
| 1 M $LiClO_4$/TTE:DME:PC (2/2/1, v/v/v) | -50 | 100 | 300, 1.5 | / | 1.91 | S5[5] |
| 0.8 M LiBF4 -0.2 M LiFSI/ PC:DME:Isobutyle acetate | -40<br>-60 | 80 | 730, 1.0<br>445, 1.0 | 4.0-4.3 | 1.7<br>1.5 | S6[6] |
| 1M LiBF4 EA/ET 7/3 v/v | -40<br>-60 | 80 | 710, 1.5<br>395, 1.5 | 2-3 | 2.15<br>1.85 | This work |

**Table S2.** The composition of Li||CF$_x$ 18650-cylinder cell

| Parts | Weight (g) | Weight Percent (w/w %) |
|---|---|---|
| Shell | 7.8 | 31% |
| Cathode | 6.5 | 25% |
| Electrolyte | 6 | 24% |
| Separator | 2 | 8% |
| Anode | 1.7 | 7% |
| Tabs | 1.5 | 6% |

## References

1 G. Cai, Y. Yin, D. Xia, A. A. Chen, J. Holoubek, J. Scharf, Y. Yang, K. H. Koh, M. Li, D. M. Davies, M. Mayer, T. H. Han, Y. S. Meng, T. A. Pascal and Z. Chen, *Nat. Commun.*, 2021, **12**, 3395.

2 S. S. Zhang, D. Foster and J. Read, *J. Power Sources*, 2009, **188**, 532–537.

3 Z. Fang, Y. Yang, T. Zheng, N. Wang, C. Wang, X. Dong, Y. Wang and Y. Xia, *Energy Storage Mater.*, 2021, **42**, 477–483.

4 J.-P. Jones, S. C. Jones, F. C. Krause, J. Pasalic, M. C. Smart, R. V. Bugga, E. J. Brandon and W. C. West, *J. Electrochem. Soc.*, 2017, **164**, A3109.

5 J. Ban, X. Jiao, Y. Feng, J. Xue, C. He and J. Song, *ACS Appl. Energy Mater.*, 2021, **4**, 3777–3784.

6 W. Xue, T. Qin, Q. Li, M. Zan, X. Yu and H. Li, *Energy Storage Mater.*, 2022, **50**, 598–605.